The Role of Inclusion on Fracture Phenomena in Separation Process in Metal Cutting

Toshiaki KANEEDA*, Hideo TSUWA**

(Received September 16, 1978)

[INTRODUCTION]

Many studies for metal cutting mechanism have been performed since Merchant's reseach. Most of them are done based on chip formation mechanism. However, from the standpoint of making much account of quality of product machined, cutting mechanism must be analysed from a viewpoint of surface generation. There have not been so many studies on this respect until now. (1)

Surface generation mechanism in metal cutting is composed of two processes. They are separation process at tool tip and burnishing process at clearance face of tool, the former is deeply concerned with surface finish. Therefore, it is very important to analyse the separation process microscopically.

The separation process is considered to be a fracture phenomenon essentially, therefore even though micro-machining with continuous chip formation, crack in separation process may damage machined surface. In this report, first, the fracture phenomena in separation process are examined in micro-machining of steel SS41 and pure aluminum A1070 with continuous chip formation. Next, effects of inclusions which initiate ductile fracture on fracture phenomena in the separation process are experimentally investigated.

In order to investigate these points mentioned above, orthogonal cutting equipment with very slow cutting speed is used.

Fracture phenomena subjected in this study are generated in micro-machining, and sizes of those are not dislocation level but larger than 1 μm.

[EXPERIMENTAL PROCEDURE]

Experimetal Techniques

Vertical milling machine is used for orthogonal cutting experiment. Work

* *Department of Mechanical Science, Okayama University of Science*

** *Department of Precision Engineering, Osaka University*

material is clamped with vice mounted on the table of the milling machine. The table of the milling machine has high accuracy and rigidity to minimise perturbations in metal cutting. The table is driven by motor separated from the milling machine to prevent from vibration and thermal effect carried from motor in the milling machine. The work material is fed traversly against the tool. In order to observe deformation geometry of cutting region during cutting, quick-stop device* with which motor is braked by generating motive power is employed.

Work Materials

Table 1. Work Material and Configuration of Tool

Work Material	Tool Material	Edge Radius at Tool Tip (μm)	Roughness at Tool Tip (Rmax μm)	Rake Angle (deg.)	Clearance Angle (deg.)
Steel SS41	High Speed Steel SKH4	3.5	1.5	15° 25° 35°	5°
Armco Iron	Tungsten Carbide P10	2.5	1.0	20°	5°
Pure Iron (99.9%)	〃	〃	〃	25°	5°
Alpha Brass BsPl	Diamond	less than 0.1	less than 0.1	20°	7°
Pure Aluminum A1070 (99.7%)	〃	〃	〃	〃	〃

Work materials used in these experiments are shown in Table 1. Pure aluminum A1070 (99.7%) is malleable (fcc metal). Carbon steel SS41 involves many inclusions and second phase (pearlite) (bcc metal). Pure iron does not involve impurities. Pure iron and armco iron do not contain second phase.

Tool Materials

Tool materials and their configurations are shown in Table 1. High speed steel (H. S. S.) SKH4 is suitable to get large rake angles and used mainly. Diamond tool is used for fine cutting of pure aluminum and α-brass. In micro-machining edge radius and roughness of tool tip influence cutting mechanism significantly, therefore tools are ground carefully and uniformly. It is considered that configurations of H. S. S. tools as well as Tungsten Carbide tools influence cutting mechanism in these experiments.

Cutting Conditions

Cutting speed is very slow 30 mm/min to minimise effects of heat generated by plastic deformation and strain rate. (2) Cutting fluids used are CCl_4 and extreme pressure oil JIS 2nd. CCl_4 is used to prevent from formation of built up edge in steel cutting. Extreme pressure oil JIS 2nd is used to prevent from overcutting

* As a result of measurement, inherent decelation distance is less than 20 μm.

in aluminum cutting. Cutting conditions are shown in Table 2.

Table 2. Cutting Conditions

Work Material	Tool Material	Cutting Speed (mm/min)	Depth of Cut (μm)	Cutting Fluid
Steel SS41	High Speed Steel SKH4	30	10 ~ 100	Partially CCl_4
Armco Iron	Tungsten Carbide P10			
Pure Iron (99.9%)	〃			
α-Brass BsPl	Diamond			—
Pure Aluminum A1070 (99.7%)	〃		10 ~ 60	Extreme Pressure Oil JIS 2nd

[EXPERIMENTAL RESULTS and DISCUSSIONS]

Origin and Shape of Crack in Steel Cutting

Separation area between bottom surface of chip and machined surface in steel SS41 cutting is observed. There exists a crack in separation area. Section of the cutting specimen is polished to investigate shape of the crack in detail. Fig. 1 shows the section of steel cutting specimen polished. The crack has been generated from tool tip

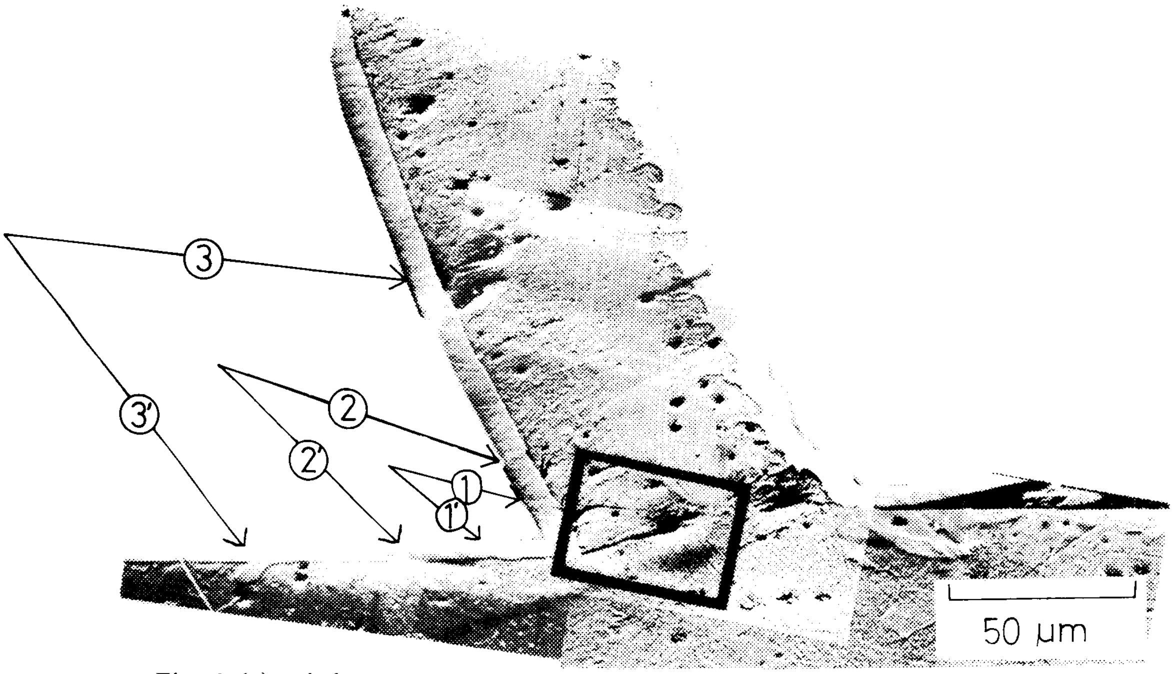

Fig. 1 (a) A large crack generated between inclusion and tool tip.

Figure 1. Scanning Electron Micrographs showing cracks in the chip. Specimen is plated by nickel and polished.

Work Material	Steel SS41	
Tool	H. S. S. SKH4	
	Rake Angle	$\alpha=25°$
	Clearance Angle	$\delta=5°$
Depth of Cut	$t_1=24\ \mu m$	
Cutting Speed	V=30 mm/min	

along shear plane as long as 40 μm. A spherical particle exists in a void near the crack tip. (Fig. 1 (a)) Observed in detail, shape of the crack is step linking a few small voids between tool tip and a void near the crack tip. At the bottom surface of

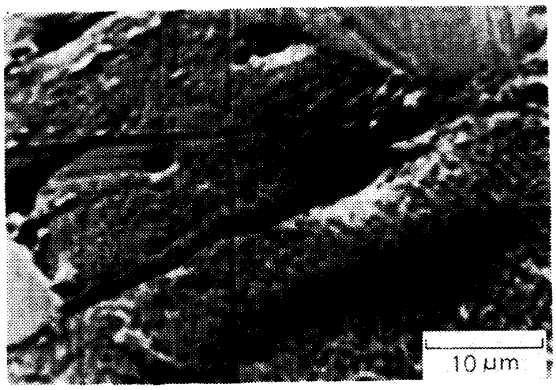

Fig. 1 (b) A higher magnification micrograph of the chip root near tool tip in Fig. 1 (a).

the chip, cracks which are considered to be generated at tool tip longer than 10μm are found, and these cracks are deformed like as a bow due to friction at rake face of tool. In the chip there are some particles and voids, around which micro-cracks have been generated by severe shear stress.

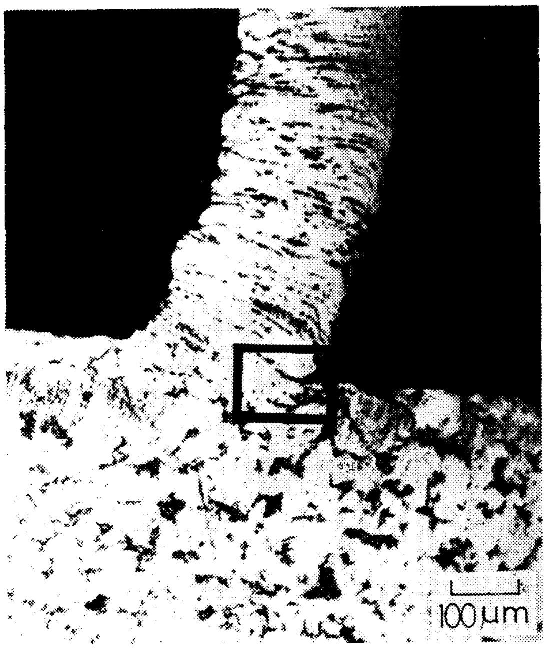

Fig. 2 (a) An optical light micrograph shows a large crack generated from tool tip along shear plane.

Fig. 2 (b) A higher magnification Scanning Electron Micrograph of the crack in Fig. 2 (a).

Figure 2. A large crack generated at the chip root.
Specimen is polished.
$t_1 = 35$ μm
Other cutting conditions are as same as Fig. 1.

As a result of analysis by Electron Probe X-ray Microanalyser (EPMA), the spherical particle in the void (see Fig. 1 (b)) is determined to be Mn-O inclusion.

Fig. 2 (a) shows a crack generated from tool tip along shear plane. Its length is about 50 μm. In this case inclusion in a void near the crack tip is found and shape of the crack is step like Fig. 1 except near the tool tip. (Fig. 2 (b)) It seems that whole shape of the crack in Fig. 2 is different from that in Fig. 1. The crack in Fig. 2, first, directs slightly downwards from tool tip, and changes its direction to upwards which is parllel to shear plane. Its bottom crosses down a plane to be cut. But these two cracks are considered to be generated with same mechanism, and the difference is only due to the time lag of the observation. That is, the crack in Fig. 1 has been generated as well as that in Fig. 2 on shape, and quick-stop device operated after cutting going forward a little in case of Fig. 1. The shape of crack in Fig. 2 corresponds to the second slip line passing through tool tip in the slip line fields. (3)

Consequently these cracks are considered to be generated along maximum shear stress direction passing through tool tip.

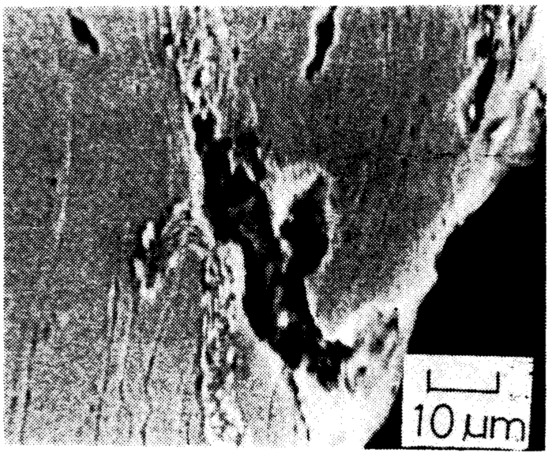

Figure 3. A void and microcrack at the bottom surface of steel chip.

Fig. 3 shows a void and microcrack at bottom surface of chip. It is revealed that a crack initiated from void propagates along boundary of pearlite (second phase) and grain boundary. Such tendency is confirmed in other steel specimens.

Schematic Diagram for Generation and Growth Process of Crack nucleated from Inclusion and Formation of Surface Damage

Fig. 4 shows schematic diagram for generation and growth process of crack nucleated from inclusion and formation of surface damage.

First, cutting is advanced, and inclusions in a work material enter plastic

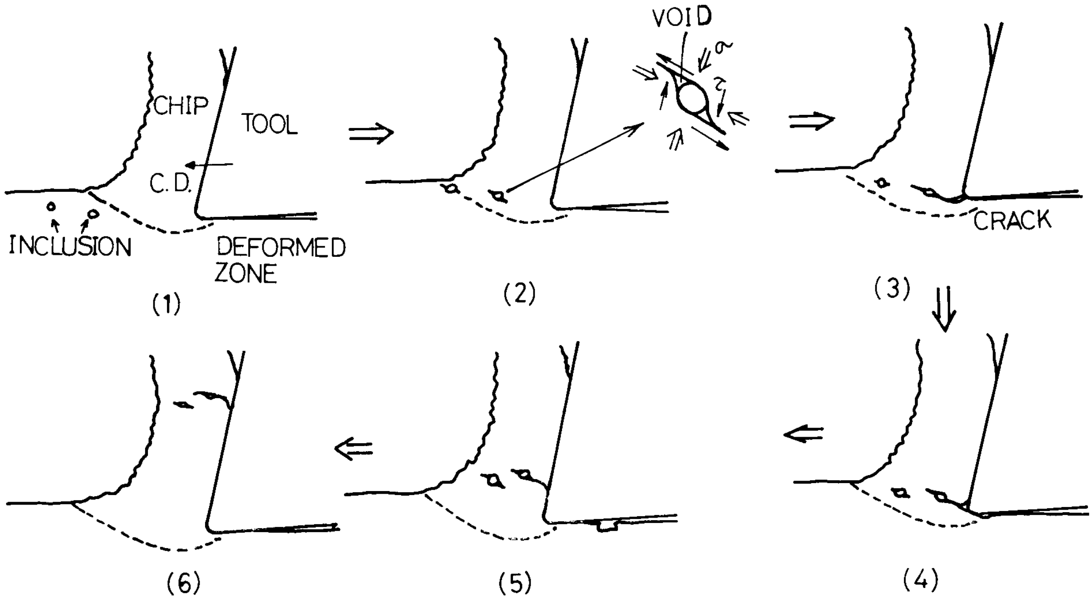

Figure 4. Schematic diagram for generation and growth process of crack nucleated from inclusion and formation of surface damage. C. D. is cutting direction.

deformation zone. (Fig. 4(1) ⟶ (2)) Inclusions act as obstacle of slip and void formations occur by pile up of many dislocations. As inclusions approach shear zone, voids grow bigger due to difference of plastic deformability between inclusions and matrix material, and microcracks are generated by severe shear stress at both side of the voids. When inclusions across shear plane, large crack is generated along second slip line (maximum shear stress direction) between the microcrack around the inclusion and tool tip. (see Fig. 4 (3)) Certainly in this case smaller inclusions or grain boundaries or second phase boundaries exist between the inclusion and the tool tip. Next process. the crack is divided into chip side and machined surface side as shown in Fig. 4 (4). The former undergoes secondary deformation at rake face of the tool and the latter is burnished by clearance face of that as shown in Fig. 4 (5). Machined surface is damaged by the crack. Furthermore the crack in the chip are deformed due to compression stress and recohesion occurs. (see Fig. 4(6))

Consequently the formation mechanism of surface damage in this case is as follows: Stress concentration around inclusion ⟶ Formation of void ⟶ Generation of microcracks by shear stress ⟶ Generation of large crack between microcrack and tool tip ⟶ Burnishing crack at clearance face of tool.

Accordingly mechanism of these fracture phenomena is considered to be deformation mode II in ductile fracture (shear mode).

Correspondence between Crack in Chip and Hollow on Machined Surface

As a crack is considered to be generated along maximum shear stress direction, machined surface is damaged actually by the crack as shown in Fig. 4 (5). In this cace the crack on the shear plane is generated along the second slip line in the slip line field. The correspondences between other cracks on the rake face side of the chip and hollows on the machined surface are confirmed as shown ①⟶①′, ②⟶②′ and ③⟶③′, in Fig. 1 (a).

After cutting experiments separation areas between bottom surfaces of chips and machined surfaces are observed. As a result of observations, the correspondences are recognised in some cases and are not recognise in other cases. These facts are due to the difference of relative situation between the inclusions and the tool tip. Fig. 5 shows

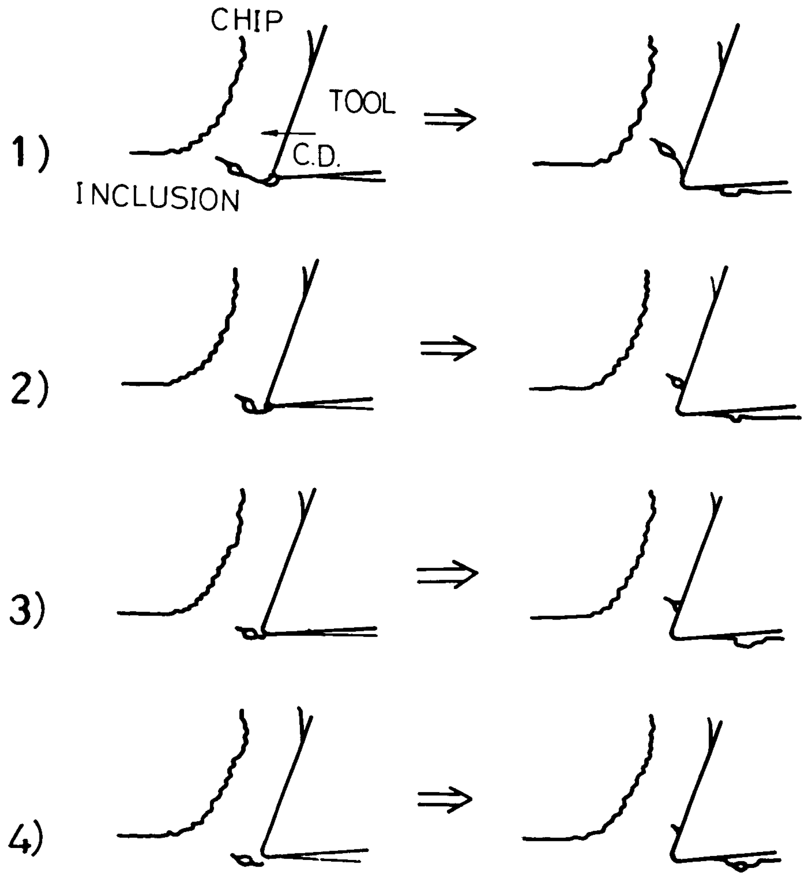

Figure 5. The difference between surface finishes damaged by fracture phenomena of various types depending on the relative position of the inclusions to that of the tool tip.

schematic diagram in which various types of damage of machined surface according to relative situation between them are shown.

Fig. 5 (1) is the case of Fig. 1. In the case of Fig. 5 (3), inclusion exists on a plane to be cut, and is broken by tool tip and machined surface is damaged. As inclusions exist not on a plane to be cut but above or below it in the case of Fig. 5 (1), (2), and

(4), machined surfaces are damaged by void formation ⟶ crack growth process. As the situation of inclusion shifts from over a plane which is to be cut to below it (Fig. 5 (1) ⟶ (4)), damage grows larger except Fig. 5 (1). These are ductile fracture, Fig. 5 (3) is deformation type I (opening mode) and the other are deformation type II in fracture (shear mode).

It is confirmed experimentally that the formation mechanism of surface damage in Fig. 5 is applied to steel, armco iron, pure aluminum, α-brass and pure copper.

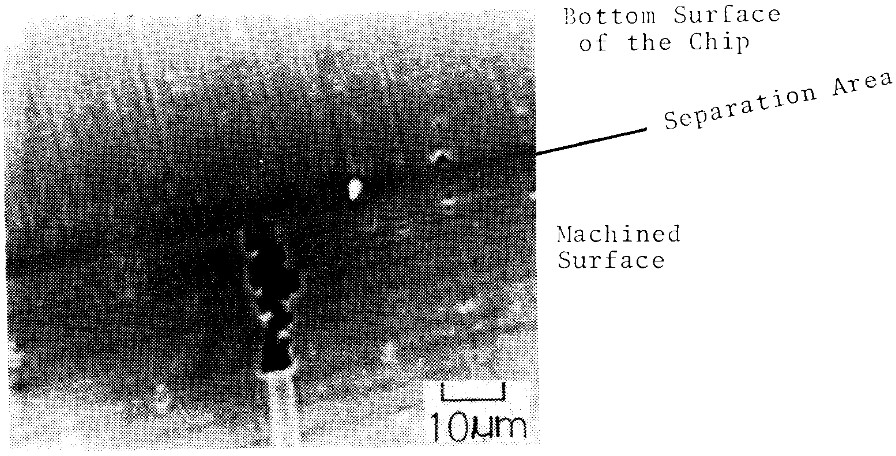

Figure 6. Scanning Electron Micrograph showing crack in the vicinity of separation area in pure aluminum cutting.
Work Material Pure Aluminum A1070 (99.7%)
Tool Diamond
$\alpha = 20°$
$\delta = 7°$
$t_1 = 25\mu m$
$V = 30mm/min$

For example, Fig. 6 shows a crack generated in the vicinity of separation area of pure aluminum specimen. Its shape is like a few ellipsoids linked and its length is about 30 μm.

Cutting speed range of the experiments mentioned above is very slow 30 mm/min. In speed range of shop machining, crack is difficult to be generated due to rise of plastic deformability associated with increase of cutting speed. Therefore, it is not decided that results mentioned above are applied to shop machining. This is a subject of study in the future.

[CONCLUSIONS]

Role of inclusion on fracture phenomena in separation process is investigated by orthogonal cutting experiment at very slow cutting speed. The results are shown as follows.

(1) Cracks are observed in separation process in micro-machining pure aluminum and α-brass of fcc and pure iron, armco iron and steel of bcc with continuous chip. Crack is nucleated from inclusions.

(2) Second phase and grain boundary in work material are a sort of source of stress concentration. Voids around inclusions and microcracks initiated from voids develop large cracks due to difference of plastic deformability along them.

(3) In case that inclusion exists on a plane to be cut, void formation $\longrightarrow$ microcrack initiation process occurs as it approaches tool tip. This fracture mechanism is deformation mode I in ductile fracture (opening mode).

(4) In case that inclusion exists over or below a plane to be cut, void formation $\longrightarrow$ microcrack initiation process occurs.

Crack is generated between the inclusion and tool tip depending on stress field, and makes surface damaged.

This is deformation mode II in ductile fracture (shear mode).

[ACKNOWLEDGEMENTS]

The authors wish to their appreciation for useful suggestions provided by Dr. Y. Namba and G. Ohmori of the Department of Precision Engineering, Osaka University.

The authors also wish to thank Wingo Limited for facilities of polishing.

[REFERENCE]

(1) for instance, Y. Kakino, Ph. D. Thesis, Kyoto University (1973).

(2) E. Usui and R. Makino, "An Example of Stress and Strain Ditributions in Slow Speed, Steady-State Machining", Journal of the Japan Society of Precision Engineering, 33, 4 (1967) 245.

(3) E. Usui, "Cutting and Grinding Mechanism I", (in Japanese) Kyoritsu Press, (1971) 74.